Composites Science and Technology 183 (2019) 107791

Contents lists available at ScienceDirect

Composites Science and Technology

journal homepage: www.elsevier.com/locate/compscitech

Fabrication of flax fibre-reinforced cellulose propionate thermoplastic composites

W. Woigk[a,1], C.A. Fuentes[b], J. Rion[c], D. Hegemann[d], A.W. van Vuure[b], E. Kramer[a], C. Dransfeld[a,2], K. Masania[a,*,1]

[a] *Institute of Polymer Engineering, FHNW University of Applied Sciences and Arts Northwestern Switzerland, CH-5210, Windisch, Switzerland*
[b] *Department of Materials Engineering, KU Leuven, B-3001, Heverlee, Belgium*
[c] *Bcomp Ltd, CH-1700, Fribourg, Switzerland*
[d] *Empa, Swiss Federal Laboratories for Materials Science and Technology, CH-9014, St. Gallen, Switzerland*

ARTICLE INFO

Keywords:
Natural fibre composite
Mechanical properties
Cellulose propionate
High toughness

ABSTRACT

Natural materials such as wood exhibit high mechanical properties through cellulose structured at multiple length scales and embedded in a matrix of similar chemical structure. These hierarchical materials have inspired the design of lightweight composites composed of naturally occurring polymers. However, the close proximity of melt and decomposition temperature remain a challenge. In this work, cellulose propionate (CP) is modified to reduce its glass transition temperature and melt viscosity, allowing its use as a matrix in a natural fibre-reinforced composite. Through better impregnation, the modified CP matrix composites showed an increase in stiffness and strength of ~10% and 20%, respectively, in comparison to unmodified CP matrix composites. The impact properties also increased by up to 28%, showing that modified CP is a credible matrix for realising sustainable all-cellulose natural fibre composites with high stiffness, strength and toughness.

1. Introduction

High-performance composites today are mostly composed of petroleum-based fibres and polymers that are energy intensive in their production and can be difficult to recycle. Naturally occurring materials such as cellulose, the most abundant bio-polymer in nature that reinforces a majority of plant cell walls [1] can be used as non-petroleum feedstock in lightweight applications that require stiffness, strength and toughness [2]. Lignocellulosic natural fibres (NF) such as flax (FF), hemp and bamboo show great potential to be used in lightweight composites due to their high specific mechanical properties and vibration damping at low environmental footprint [3–5]. For applications that require high mechanical performance, NF-reinforced composites are typically composed of thermoset matrices due to their high cost-to-performance ratio and relative ease of processing, which however, limits their recycling. To overcome this challenge, all-cellulose composites (ACC), consisting of only reinforcing phase [6] or those in which both the reinforcement and the matrix are composed of cellulose, have been of great interest [7–12]. Similarity in the chemical nature of fibre and matrix can promote stress transfer and offer high stiffness and strength [7,13,14] while remaining recyclable [15]. Typically, this has been achieved by complete [13,16] or partial dissolution of the cellulose [7,9,12] which usually involve harmful solvents, yet lead to composites with excellent in-plane alignment at the detriment of the transverse mechanical properties. A method of tailoring the in-plane properties is to produce composites via stacking and hot pressing of NF-preforms and alternating thermoplastic polymer films [17]. Polymers such as cellulose acetate, cellulose acetate butyrate and cellulose propionate (CP) are therefore highly attractive as alternative cellulose based matrix materials. Of those, CP presents the stiffest and toughest polymer. However, the close proximity of their melting and decomposition temperatures and their high melt viscosities means that processing composites without degradation of one of the phases is a challenge. During composite processing, their high viscosities would require either very high pressures or long impregnation times. The potential high pressures could break the fibre's microstructure leading to reduced flexural and interlaminar strength, or induce fibre washing [18,19], whereas high temperatures would cause fibre degradation. For

---

[*] Corresponding author.
E-mail address: kunal.masania@mat.ethz.ch (K. Masania).
[1] Current address: Complex Materials, Department of Materials, ETH Zürich, CH-8093, Zurich, Switzerland.
[2] Current address: Aerospace Manufacturing Technologies, Faculty of Aerospace Engineering, Delft University of Technology, Kluyverweg 1, 2629 HS Delft, the Netherlands.

https://doi.org/10.1016/j.compscitech.2019.107791
Received 18 January 2019; Received in revised form 25 June 2019; Accepted 26 August 2019

the enticing case of cellulose NF-reinforced cellulose matrix composites, the combination of bio-based polymers and utilisation of short impregnation distances through the thickness could allow the fabrication of bio-based, all-cellulose engineering composites. In order for the cellulose based polymers to be suitable as film stacking matrix material, modifications of polymer structure are necessary to reduce the melt viscosity sufficiently, to enable fibre impregnation.

The development of a modified cellulose propionate (CP) matrix material that separates the material's melt and decomposition temperatures and demonstrates reduced melt viscosity could allow for natural fibre composite processing without the degradation of the constituents and therefore lead to enhanced mechanical properties. The effect of plasticiser and slip agent on the thermal, mechanical, surface energy and rheological properties was systematically studied. The most promising polymer-additive composition was then used to produce composites; characterising the flax fibre wetting, flexural and impact properties of the composites in the longitudinal and transverse directions.

2. Materials and methods

2.1. Materials

Continuous fibre reinforcement was introduced in the form of unidirectional ampliTex™ UD type 5009 flax fibres (Bcomp, Switzerland) to manufacture FF-composites. The fibre preforms were cut (150 × 90 mm) and dried in a vacuum oven at 110 °C and 20 kPa for 15 min prior to composite processing.

A bio-based cellulose ester polymer, cellulose propionate (Cellidor CP-400), abbreviated CP, was purchased from Albis Plastic GmbH (Germany). A non-phthalate 1,2-Cyclohexane dicarboxylic acid, diisononyl ester plasticiser (Hexamoll DINCH, BASF, Germany) and a fatty amide (C22 mono-unsaturated erucic acid amide) slip agent (Erucamide, Abril, UK) were combined within the CP to modify the material's thermal and rheological properties and its wetting behaviour on a substrate. Fig. 1 shows the chemical structures of the compounds used in this study. The CP is a cellulose derivative that is reacted with propanoic acid to form an organic ester that has a low density, high stiffness, excellent impact properties, but high melt viscosity. The physical properties of polymers may be altered by solvation of plasticisers between the molecular chains of the base-polymer, leading to a reduced chain interaction and entanglement. Slip agents also behave as plasticisers, however, are less soluble between the polymer chains and thus are intended to be more surface active and aid processing by reducing frictional effects with metallic surfaces of a die or extruder. To reduce the viscosity, plasticiser and slip agent contents of 0, 5, 10, 15 wt% and 0, 1, 2, 3 wt%, respectively, were considered. The resulting materials are denoted as HexX and EruY where X and Y are weight% concentrations of Hexamoll and Eurcamide.

Polypropylene (PP), type 515A, a medium isotactic PP homopolymer, supplied by Sabic (Saudi Arabia) and the epoxy resin (EP), Araldite LY5052, a two-molecule mixture resin with Aradur 5052, a six amine molecule hardener, with a resin-to-hardener weight ratio of 100:38, supplied by Huntsman Advanced Materials (Basel, Switzerland) were used as reference matrix materials for comparison with the developed CP matrix FF-composites.

The contact angle analysis were carried out with analytical grade test liquids, ultrapure water: 18.2 Ω cm resistivity, diiodomethane ≥99% (Acros, Fisher Scientific, USA), and ethylene glycol ≥99% (Sigma–Aldrich, Merck, USA).

2.2. Rheological measurements

The complex viscosity of polymers was measured using a Physica MCR 300 (Anton Paar, Buchs, Switzerland). The polymers were heated to 190 °C and measured using a plate-plate method (25 mm diameter plate) at frequencies between 0.1 and 100 Hz with a gap size of 1.6 mm to avoid slippage at the plate polymer interface.

2.3. Polymer processing

The material combinations were pre-mixed by adding the plasticiser and slip agent mass contents to the raw CP granulates using a Brabender mixer for the pure polymer trials, and combined with the pellets using a standard blender. Pre-mixed materials were compounded batch-wise in a Leistritz (Germany) twin-screw extruder. Thermoplastics films were produced using a Collin (Dr. Collin GmbH, Germany) Teach Line single-screw extruder equipped with a film die. Films were drawn from the die using a water-cooled pulling unit which was set to 50 °C before winding the films onto cardboard cylinders. 60 mm wide and ∼0.2 mm thick films were drawn from the extrusion machine to allow for the film stacking of FF-composites at fibre fractions of 50 vol%.

2.4. Contact angle measurement and surface energy analysis

Advancing and receding contact angles of various test liquids of analytical grade (ultrapure water, diiodomethane, and ethylene glycol) were measured on the polymer films and flax technical fibres at 20 °C and 50% relative humidity on a Krüss K100 SF tensiometer using the Wilhelmy technique [20] with detailed description in Ref. [17].

To reduce the effect of liquid absorption by the technical fibres during wetting measurements, fibres were carefully selected by means of optical microscopy, ensuring the fineness of the fibre measuring less than 50 µm, which typically corresponds to 2 or 3 elementary fibres, and that technical fibres were in a compact state without the presence of loose elementary fibres. The weight of the fibre was measured before and after the test to estimate the mass related to sorption. Fibre samples with a weight increment greater than 10%, which corresponds to a variation of ∼2° contact angle of water on flax, were neglected from the measurement set. Surface energy components were calculated according to the Van Oss model using Equation (1), where the relation between the surface energy components of different liquids and a solid

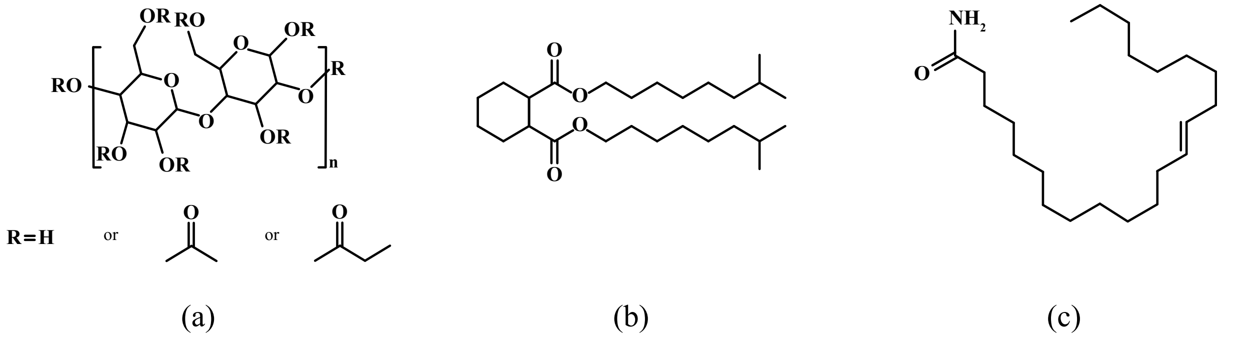

(a) (b) (c)

Fig. 1. Chemical structures of (a) Cellulose propionate thermoplastic polymer, (b) Hexamoll DINCH (plasticiser) and (c) Erucamide (slip agent) additives.

with respect to the contact angle, θ, is given in its matrix notation. SurfTen 4.3 software [21] was used to evaluate Equation (1).

$$Ax = b \tag{1}$$

where

$$\boldsymbol{A} = \begin{bmatrix} \sqrt{\gamma_{l,1}^{LW}} & \sqrt{\gamma_{l,1}^{+}} & \sqrt{\gamma_{l,1}^{-}} \\ \sqrt{\gamma_{l,2}^{LW}} & \sqrt{\gamma_{l,2}^{+}} & \sqrt{\gamma_{l,2}^{-}} \\ \cdots & \cdots & \cdots \\ \sqrt{\gamma_{l,m}^{LW}} & \sqrt{\gamma_{l,m}^{+}} & \sqrt{\gamma_{l,m}^{-}} \end{bmatrix}, \qquad \boldsymbol{x} = \begin{bmatrix} \sqrt{\gamma_{s}^{LW}} \\ \sqrt{\gamma_{s}^{-}} \\ \sqrt{\gamma_{s}^{+}} \end{bmatrix}, \qquad \boldsymbol{b} = \begin{bmatrix} \gamma_{l,1}(1+\cos\theta_1)/2 \\ \gamma_{l,2}(1+\cos\theta_2)/2 \\ \cdots \\ \gamma_{l,m}(1+\cos\theta_m)/2 \end{bmatrix}$$

$\gamma_{s,l}$ are the solid and liquid surface energy, respectively, $\gamma_{s,l}^{LW}$ represents the Lifshitz-van der Waals component, $\gamma_{s,l}^{+}$ represents the acidic and $\gamma_{s,l}^{-}$ the basic component.

The solid-liquid interfacial energy, γ_{sl}, and the work of adhesion, W_a, could subsequently be calculated according to the following equations:

$$\gamma_{sl} = \left(\sqrt{\gamma_s^{LW}} - \sqrt{\gamma_l^{LW}}\right)^2 + 2\left(\sqrt{\gamma_s^{+}} - \sqrt{\gamma_l^{+}}\right)\left(\sqrt{\gamma_S^{-}} - \sqrt{\gamma_l^{-}}\right) \tag{2}$$

$$W_a = \gamma_s + \gamma_l - \gamma_{sl} \tag{3}$$

2.5. Micro-computed tomography

A Phoenix NanoTom X-ray computed tomography equipment (General Electric Company, Fairfield, USA) and a SkyScan micro computed tomography (μCT) device (Bruker microCT, Kontich, BE) were used in order to evaluate the void content of 2 × 2 mm cross-section composite bars prepared using Accutom-100 (Struers GmbH, Germany) cutting machine. The applied voltage and current were 60 kV and 240 μA, respectively, using a molybdenum source. The exposure time was 500 ms and a frame averaging of 4 and image skip of 1 was applied. The obtained voxel size was 1.25 μm. For image processing and analysis, the 2D/3D image analysis software CTAn (v.1.16) was used. The 3D volume measurement of every single pore is based on the marching cubes volume model. For visualisation in 3D space, CTVol (v.2.3) software was used.

2.6. Composite manufacturing

Unidirectional thermoplastic FF-composites were manufactured via direct impregnation by stacking the required amount of polymer films on top of the fibre preform, or interleaved polymer film stacking. Pre-dried fabrics were stacked in a steel mould to press coupons of ~2 mm thickness with fibre content of 50 vol%. The closed mould was placed in a P200T-2E (Vogt, Germany) laboratory press, pre-heated to 190 °C. After 10 min for thermal normalisation, a cavity pressure of 1 MPa was applied followed by transfer to a cooling unit for ~10 min to cool to room temperature whilst maintaining the pressure. In accordance with the impregnation times calculated using Darcy's law, direct impregnated CP and mod_CP matrix FF-composites were processed for 50 and 712 min, respectively, whereas the film stacking dwell time was set to 10 min. Thus, in total, four CP matrix FF-composite combinations were manufactured. The EP matrix FF-composites were produced via compression resin transfer moulding [22,23], utilising a suitable cure cycle of 24 h at room temperature. Test specimens were cut using a DIADISC 5200 (Mutronic Präzisionsgerätebau GmbH & Co. KG, Rieden, Germany).

2.7. Thermo-analytical and mechanical characterisation

Differential Scanning Calorimetry (DSC) was performed to study the effect of the plasticiser and slip agent content on the glass transition temperature, T_g, using a TA Q1000 apparatus (New Castle, New Jersey, USA). Two heating cycles were used to measure the T_g of each polymer, whereby each sample was first heated to 190 °C, cooled to 0 °C, followed by a second heating to 190 °C using ramps of 10 °C/min. The T_g was extracted from the second heating cycle. Samples of about 5 mg were used. Dynamic Mechanical Analysis (DMA) was carried out on a TA Q800 apparatus (New Castle, New Jersey, USA) at temperature of 25 °C. Measurements of 35 × 10 × 1 mm specimens were taken at a frequency of 1 Hz and amplitude of 40 μm. Tensile tests on bulk polymers and flexural test on composites were carried using a universal testing machine (walter + bai AG, Löhningen, Switzerland) equipped with a 100 kN and 1 kN capacity load cells, respectively. Both tests were carried out on dog-bone shaped samples (specimen type 1A according to DIN EN ISO 527-2), whereas in the flexural tests only the sample's middle part with a constant cross-sectional area was of relevance. The specimens were loaded at a constant displacement rate of 50 mm/min for tension and 2 mm/min for flexure. Deformations were recorded using a clip-on extensometer and a linear variable differential transformer. Charpy impact tests were conducted on a Zwick 5102 Charpy impact testing machine (Zwick GmbH & Co. KG, Ulm, Germany). Pendulums of capacity 7.5 J for the bulk polymers, 1 J for longitudinal and 0.5 J for transverse FF-composites were used. Frictional effects were removed by a specimen-free calibration. Bulk polymer and composite samples had a size of 80 × 10 × 4 mm and 50 × 10 × 2 mm, respectively, in accordance with DIN EN ISO 179-1. Support spans of 62 and 20 mm were used for polymer and composite testing, respectively. In the notched samples, a machined v-shaped notch was sharpened via drawing of a sharp blade followed by tapping.

3. Results

3.1. Rheological behaviour of CP compositions

Whilst adding plasticiser and slip agent can decrease the viscosity and potentially accelerate the impregnation process, the mechanical properties are detrimentally affected because additives with lower mechanical performance are introduced to decrease molecular entanglement of the CP. Therefore, a material combination offering a reasonable processing viscosity whilst retaining the mechanical properties such as stiffness and strength was sought.

Fig. 2 shows frequency sweep measurements performed to study the rheological behaviour of the individual CP compositions and to account for a broader range of shear rates that may occur during thermoplastic polymer and composite processing. Fig. 2 (a) and (b) show individually the viscosities for varying slip agent and plasticiser contents, respectively. Generally, it can be seen that the CP viscosities decrease with increasing frequency, which indicates a shear-thinning behaviour of the CP. Furthermore, one can see that the CP viscosity can be reduced by both additives. In the tested weight content range, the Hexamoll (Fig. 2 (b)) has clearly a larger effect on the viscosity than the Erucamide (Fig. 2 (a)). The addition of more than 2 wt% Erucamide did not further decrease the viscosity, suggesting saturation of the surface-active components in the CP compositions. Viscosity reduction due to the addition of Hexamoll did not reach a plateau value for the compositions studied.

Fig. 2 (c) and (d) show the melt viscosities for Erucamide concentrations at 5 wt% and 10 wt% of Hexamoll in the CP compositions, respectively. When adding both plasticiser and slip agent, the characteristic effects of each additive were transferred to the material combination. For example, the 5 wt% of Hexamoll reduced the viscosity significantly, whereas the addition of 1, 2 and 3 wt% of Erucamide contributed only marginally to a further reduction in viscosity. The same holds true for compositions with 10 wt% of Hexamoll, whereas the initial drop is clearly higher due to the higher plasticiser content. The saturation effect when adding 3 wt% of Erucamide could also be recorded for additive combinations.

3.2. Polymer properties

Fig. 3 (a) and (b) show in surface plots the effects of the additives on

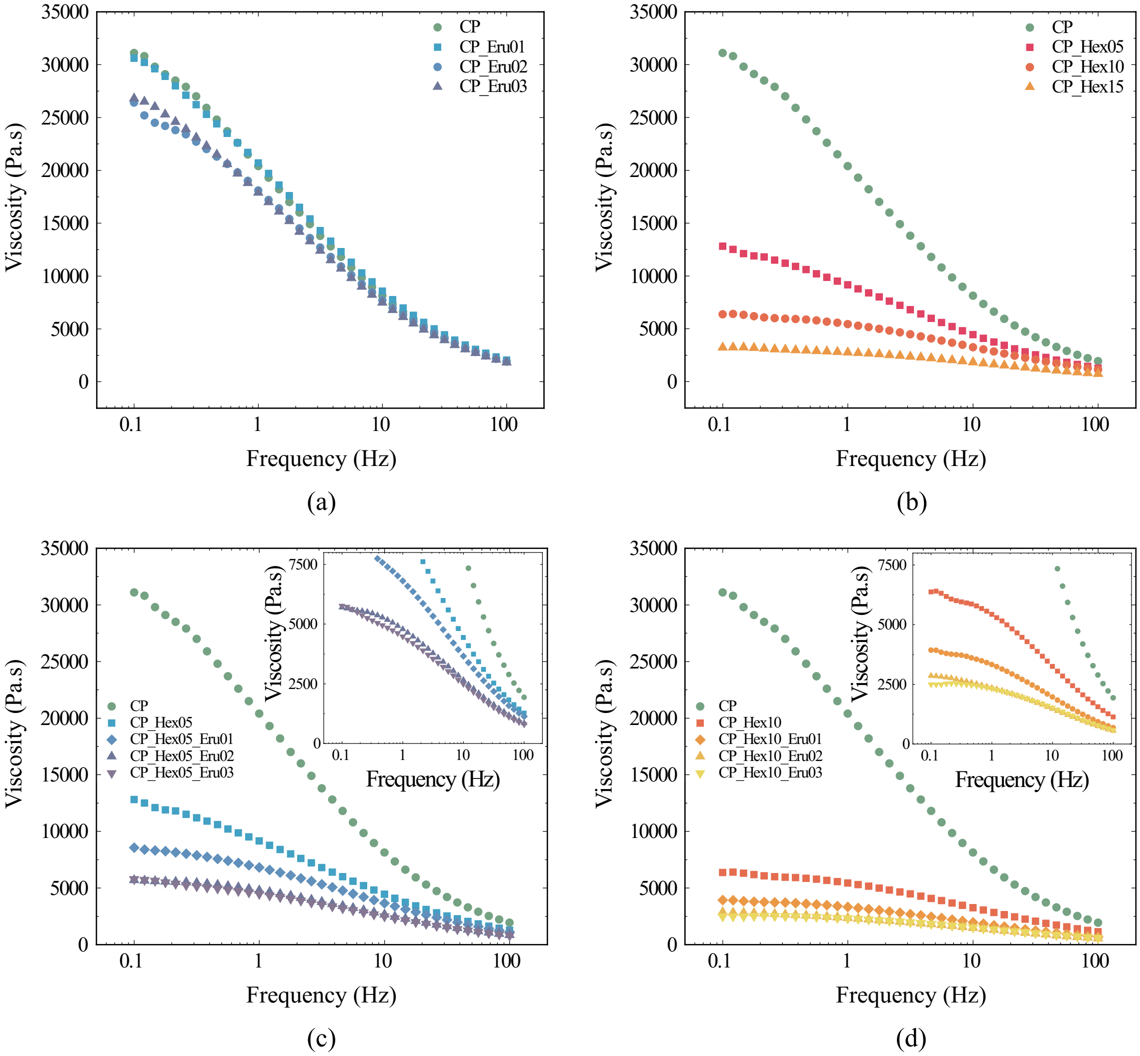

Fig. 2. Melt viscosity versus frequency of CP compositions at 190 °C for (a) Erucamide blends, (b) Hexamoll blends, (c) 5 wt% Hexamoll (Hex05) varying Erucamide content, and (d) 10 wt% Hexamoll (Hex10) varying Erucamide content.

the glass transition temperature, T_g, and the storage modulus, E', of CP. The T_g of CP was measured to be 121 °C. With the addition of 10 wt% of plasticiser, the T_g was reduced to 102 °C, while the addition of 2 wt% of slip agent decreased the T_g to 116 °C. 10 wt% of Hexamoll reduced E' to 1.5 GPa, whereas with 2 wt% of Erucamide, E' was compromised only slightly down to 1.7 GPa, compared to 1.8 GPa for pure CP. A material combination that showed the desired reduction in the melt viscosity at low frequency with acceptable compromise in T_g and E' is the CP_Hex10_Eru02 (further referred to as mod_CP) composition. T_g and E' of mod_CP were measured to 108 °C and 1.4 GPa, respectively, being reductions in T_g of 10% and in E' of 21% compared to CP.

Fig. 4 (a) shows the tensile stress-strain curves for CP, mod_CP and the reference materials EP and PP. Young's moduli for EP, PP, CP and mod_CP were found to be 3.3, 1.7, 1.6 and 1.3 GPa, respectively. The strengths were measured to 63, 35, 39 and 28 MPa. Epoxy as high-performance thermoset polymer has clearly an advantage over thermoplastic polymers considering stiffness and ultimate tensile strength. However, the highly cross-linked nature of EP impedes extensive plastic deformation, causing brittle material behaviour with maximum strain to failure of ~3%. Contrarily, the thermoplastic polymers have the ability to undergo very large plastic deformations without significant load shedding. The CP and mod_CP exhibit a strain-hardening effect after reaching the maximum stress followed by a small drop in the load. Interestingly, despite the reduction in modulus and strength for the mod_CP, the strain-hardening material behaviour seems not to be affected by the introduction of the additives.

Fig. 4 (b) shows the unnotched (blue bars) and notched (green bars) Charpy impact strength. The unnotched impact strength of CP and the mod_CP were measured to 192 and 195 kJ/m^2, respectively, which represents a ~7-times and ~3-times higher impact strength compared to EP and PP, respectively. Notched CP and mod_CP strengths of 8.5 and 16.3 kJ/m^2 were measured. As expected, the impact strengths of the notched samples are considerably lower due to the notch effect and associated stress concentrations. Similar to the unnotched properties, the impact strength of the CP specimens was measured to be ~3-times higher than EP and PP. Interestingly, the notched strength of mod_CP is twice as high as the strength of CP, and ~6-times higher than EP and PP. The high notched impact strength of mod_CP suggest a lower sensitivity to notches due to the addition of plasticiser and slip agent.

3.3. Surface energy analysis

Table 1 shows the averages of the measured advancing and receding contact angles, and the calculated equilibrium angles for the polymer films, as well as the advancing angles for flax fibres. In Table 2, the surface energy components of the thermoplastic surfaces and flax fibre, calculated using the angles shown in Table 1, are presented. As expected, PP exhibits the lowest polar surface energy components, since

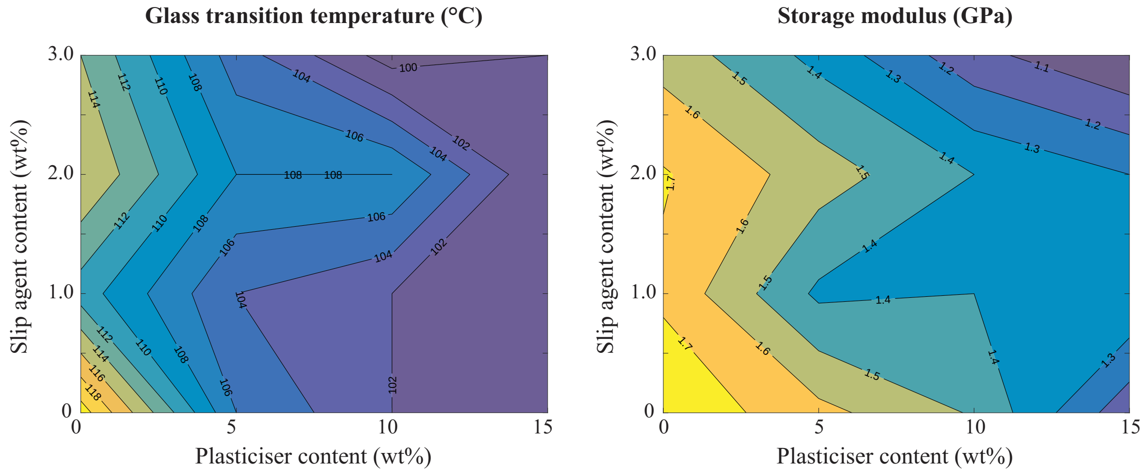

(a) (b)

Fig. 3. Effect of plasticiser (Hexamoll) and slip agent (Erucamide) contents on the polymer properties: Surface diagrams of (a) glass transition temperature and (b) storage modulus as a function of the plasticiser and slip agent contents.

pure PP is a non-polar polymer. Although pure PP should exhibit a null polar component, the effect of aging processes, as well as contamination and oxidation, can produce a deviation from the theoretical magnitude of the polar components [24]. On the contrary, both CP and mod_CP have high and similar total surface energies due to the presence of functional groups: hydroxyl (-OH), carbonyl (-$COCH_3$) and ester (-$OCOCH_3$), which increases mainly the basic polar component and results in polymers also showing high Lifshitz-Van Der Waals (LW) components.

The surface composition of flax fibres is known to be more complex, with different functional groups present on their surface [25,26]: aliphatic or aromatic carbon participating in LW interactions, as well as C-OH, C–O–C = O, O–C–O, COOH, COOC and COOH groups lending polar surface behaviour to flax fibres, which is in agreement with the surface energy estimations. The calculated theoretical work of adhesion between flax fibre and the thermoplastic matrices suggests that a better adhesion may be expected for the CP polymers compared to PP.

3.4. Quantitative fibre impregnation of FF composites

The order of magnitude in time for impregnation, t_{impreg}, for the case of a one-dimensional, saturated, isothermal fluid flow under constant pressure was calculated with Darcy's law [27]:

$$t_{impreg} = \eta \frac{(1-v_f)L^2}{2\,\kappa\,\Delta P} \tag{4}$$

where η is the melt viscosity, v_f the fibre volume fraction, L the impregnation length, κ the permeability and the impregnation driving pressure difference. The model was deemed sufficient due to negligible dynamic wetting through capillary forces of the high viscosity melt [28]. To qualitatively compare the modified polymers, using a conservative value of $\kappa = 10^{-11}$ m^2 [29], the model was used to determine the effect of the melt viscosity and impregnation length on the theoretical impregnation time. The pressure difference, , was calculated as

$$\Delta P = P_{apl.} - P_c - P_{atm.} \tag{5}$$

where $P_{apl.}$ is the applied pressure during processing, P_c the capillary pressure acting in the porous medium and $P_{atm.}$ the atmospheric pressure. Since P_c was assumed to be zero, was calculated as the difference between applied and atmospheric pressure.

Fig. 5 (a) and (b) show in double-logarithmic plots the calculated impregnation times as function of the melt viscosity for half a layer and

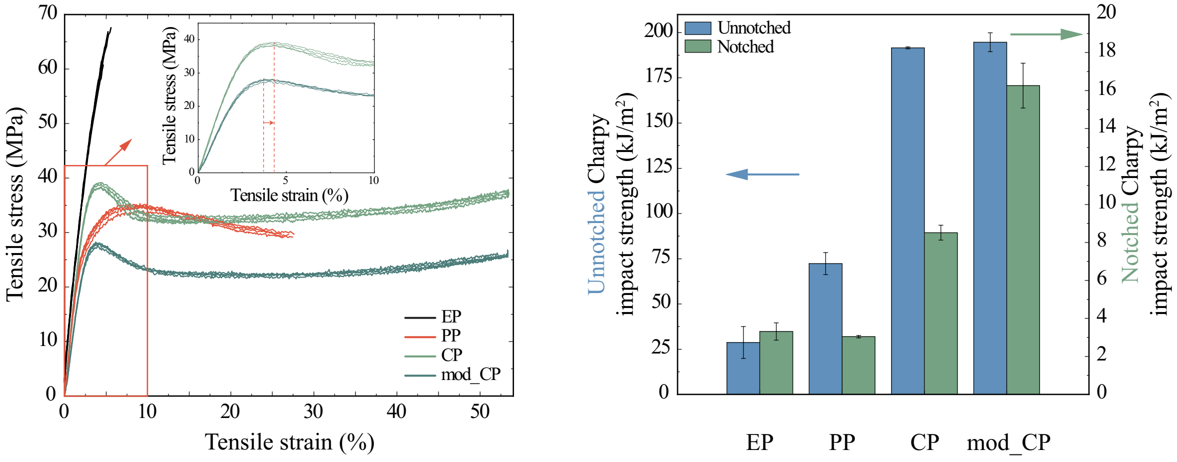

(a) (b)

Fig. 4. Polymer properties of modified CP (mod_CP) in comparison with CP and EP and PP: (a) Tensile stress-strain-diagram, the inset illustrates the reduction in strain at maximum stress for mod_CP, (b) Charpy impact strength for unnotched (blue bars) and notched (green bars) polymers. (For interpretation of the references to colour in this figure legend, the reader is referred to the Web version of this article.)

Table 1
Advancing, receding and equilibrium contact angles of probe liquids on flax and thermoplastic surfaces: water (WT), diiodomethane (DM) and ethylene glycol (EG).

Liquid	WT			DM			EG		
	adv	rec	equ	adv	rec	equ	adv	rec	equ
Flax fibre	52.6 ± 4.4	–	–	60.2 ± 4.3	–	–	45.0 ± 5.6	–	–
PP	98.2 ± 0.9	78.1 ± 1.1	88.2 ± 1.0	69.5 ± 0.9	45.6 ± 1.2	58.3 ± 1.0	73.3 ± 0.2	54.6 ± 0.3	64.3 ± 0.2
CP	82.4 ± 0.4	55.6 ± 0.2	69.6 ± 0.3	53.1 ± 0.3	29.9 ± 0.4	42.8 ± 0.3	55.3 ± 0.2	27.9 ± 0.3	43.4 ± 0.2
mod_CP	93.7 ± 1.1	54.2 ± 0.9	74.9 ± 1.0	58.2 ± 0.4	16.6 ± 0.5	42.0 ± 0.4	70.4 ± 1.2	34.8 ± 1.1	54.6 ± 1.1

six layers of flax fibres, representing film stacking and direct impregnation, respectively. The estimated impregnation time of 0.35 min for half a layer of FF using the mod_CP represents a significant reduction compared to the impregnation with CP. According to Equation (4), the mod_CP allows for a ~17-times faster impregnation in the film stacking process. A similar trend was observed for the six-layer direct impregnation process, in which the mod_CP impregnates the fibre stack ~14-times faster than CP. The plots show that there is a considerable reduction in melt viscosity of more than one order of magnitude due to the introduction of additives into CP polymer.

3.5. Composite morphology

Fig. 6 shows the three-dimensional reconstruction of typical CP (top row) and mod_CP (bottom row) matrix FF-composites produced via film stacking. The figure depicts the porosity distribution in three different perspectives. Total porosities of 0.57 ± 0.03% and 0.20 ± 0.01% were measured for the CP and mod_CP matrix FF-composites, respectively. As can be seen in Fig. 6, porosity is mainly located inside the yarns with an in-plane orientation of voids along the yarn axis. The CP matrix FF-composites have a porosity that is almost three-times higher than in the mod_CP FF-composites. Accordingly, the modification of CP seems to influence the impregnation and formation of voids during composite processing, allowing the polymer to better penetrate inside the yarn and in between technical fibres.

3.6. Composite quasi-static flexural properties

Fig. 7 shows the flexural stress-strain curves for CP and mod_CP matrix FF-composites tested in (a) longitudinal and (b) transverse directions and the corresponding specimens with a focus on the damage zones. As calculated using Darcy's law (Equation (4)) for direct impregnation, the CP and mod_CP matrix FF-composites were processed for 712 and 50 min, respectively. Longitudinal flexural moduli of 22 and 24 GPa were measured for film stacked CP and mod_CP matrix FF-composites, whereas 16 and 18 GPa were measured on the direct impregnated composites, respectively. Strengths of 174 and 205 MPa could be determined for film stacked CP and mod_CP matrix FF-composites, whereas direct impregnated samples measured values of 155 and 185 MPa, respectively. Those numbers represent a relative increase in modulus of ~10 and 13% for CP and mod_CP matrix FF-composites when using the film stacking process instead of direct impregnation. The strengths of film stacked composites were found to be enhanced for both materials by ~20% compared to direct impregnated composite properties.

From optical images of CP matrix FF-composites (orange indicated sample) dry fibres were observed in the fibre tows. Imperfect fibre impregnation may cause local instability, particularly in compression, which allows for the development of kink bands, without obvious damage on the tensile side of the specimen. Contrarily, the mod_CP matrix FF-composites exhibit a combination of kink band formation (compressive failure) and fibre bundle pull-out (tensile failure), indicative of better stress transfer due to better impregnation. In addition, the sharp load drop in the stress-strain curves (red and dark blue curves in Fig. 7 (a)) indicates a change in the failure behavior from a gradual for film stacked to a sudden load shedding for direct impregnated composites.

In the transverse direction (Fig. 7 (b)), average moduli of 1.9 and 2 GPa were measured for film stacked CP and mod_CP matrix composites, whereas directly impregnated materials reached moduli of 1.4 and 1.9 GPa, respectively. This is an increase in modulus of film stacked over direct impregnated composites of 36 and 5% for CP and mod_CP matrices. The strengths were measured to 22 and 26 MPa for film stacked CP and mod_CP matrix composites, and to 15 and 23 MPa for the direct impregnated composites, respectively, which is an increase of 47 and 13%, respectively. It was found that failure initiation on transverse samples was governed by matrix yielding. Indications for this mode are the vertical, delta-shaped white damage zones and gradual load shedding, which is a typical matrix failure behaviour. More pronounced damage can be seen on the direct impregnated CP (red) and mod_CP (dark blue) matrix FF-composites, both showing a cracked tensile side. The fracture surface, analysed with optical microscopy, reveals minor transverse fibre failure, but mostly fibre matrix debonding.

Fig. 8 (a) and (b) show flexural stress-strain curves of representative samples for film stacked CP and mod_CP matrix FF-composites, tested in longitudinal and transverse flexural directions. In order to better distinguish the two sets of graphs, a horizontal offset of 1% was added to the curves of the mod_CP matrix FF-composites. Interestingly, although the bulk matrix properties of mod_CP were inferior to CP, the mod_CP matrix FF-composite properties in the longitudinal fibre direction could be enhanced. This suggests that longitudinal properties are also influenced by fibre volume fraction, impregnation quality and void content. The lower transverse modulus for CP matrix FF-composites indicates poor fibre wetting, which would then also explain the reduced transverse strength. This is confirmed by the μCT results in Fig. 6. Since both the matrix strength for CP and the predicted work of adhesion for CP are higher than for mod_CP, the reduced transverse strength is likely attributed to poor fibre wetting.

The CP and mod_CP matrix FF-composite properties are compared to those of EP and PP matrix FF-composites in Fig. 9. The longitudinal modulus of the EP matrix FF-composites was measured to be 27 GPa, which is comparable to 24 GPa for the mod_CP matrix FF-composites. A

Table 2
Surface energy components of flax and thermoplastic films and work of adhesion, W_a, taking flax as substrate.

Material	γ^{LW} (mJ/m^2)	γ^{-} (mJ/m^2)	γ^{+} (mJ/m^2)	γ^{tot} (mJ/m^2)	W_a (mJ/m^2)
Flax fibre	28.5 ± 2.4	16.7 ± 3.0	0.67 ± 0.47	35.2 ± 3.6	–
PP	29.6 ± 0.6	1.7 ± 0.3	0.04 ± 0.02	30.1 ± 0.6	61.9 ± 4
CP	38.2 ± 0.2	5.24 ± 0.1	0.2 ± 0.02	40.2 ± 0.2	73.4 ± 3.8
mod_CP	38.6 ± 0.3	4.1 ± 0.4	0.001 ± 0.0	38.7 ± 0.4	69.8 ± 3.9

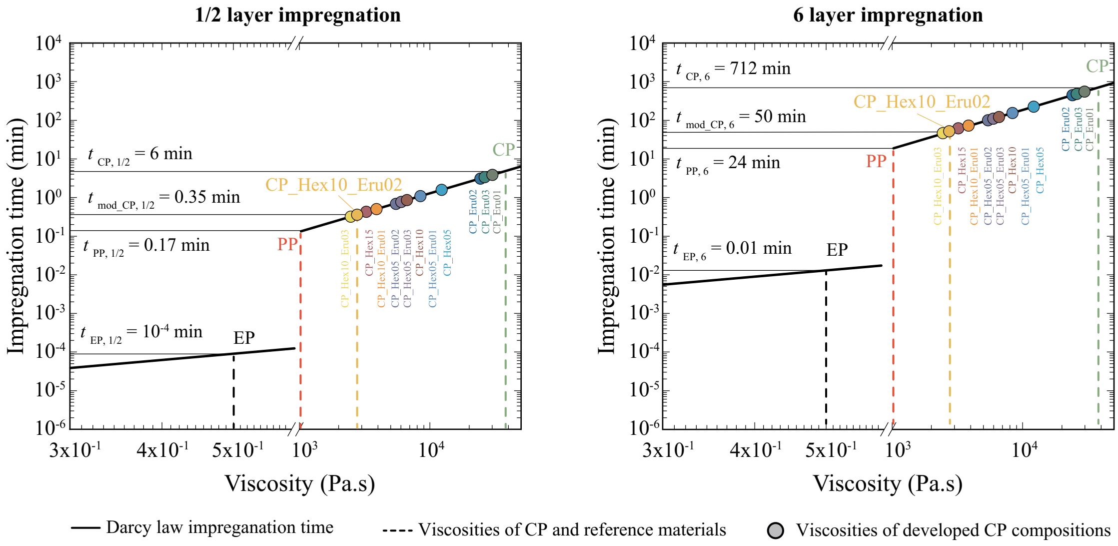

(a) (b)

Fig. 5. Impregnation times as a function of processing viscosity for (a) film stacking and (b) direct impregnation process.

bigger difference was measured for the strength, which is 337 MPa for EP and 205 MPa for mod_CP matrix FF-composites.

The flexural modulus and strength of the EP matrix FF-composites samples tested in transverse fibre direction were measured to be 2.6 GPa and 39 MPa, whereas the mod_CP matrix FF-composites measured a modulus of 2.1 GPa and strength of 26 MPa.

3.7. *Composite Charpy impact properties*

Fig. 10 (a) and (b) show the unnotched and notched Charpy impact properties in the longitudinal and the transverse direction, respectively. In the longitudinal direction, the unnotched impact strength of the mod_CP matrix FF-composites were measured to 59.6 kJ/m^2, which is ~30% higher than values for EP and CP matrix FF-composites. As expected, the notched longitudinal samples reached lower effective values. EP, PP and CP matrix FF-composites exhibited similar properties, while composites with the mod_CP matrix showed a slight enhancement over the other materials. This may be explained by a combination of failure modes. The mod_CP matrix FF-composites exhibited fibre failure and compression kink bands, which were found to be characteristic failure modes for either EP or thermoplastic FF-composites.

In the transverse direction, the composites with the thermoplastic matrices reached significantly higher values compared to the EP matrix FF-composites, above all, the mod_CP matrix FF-composites reached the highest unnotched strength of 4.4 kJ/m^2. The EP matrix is not able to dissipate energy through plastic deformation, which leads to the low toughness and is responsible for the brittle failure of the composite with

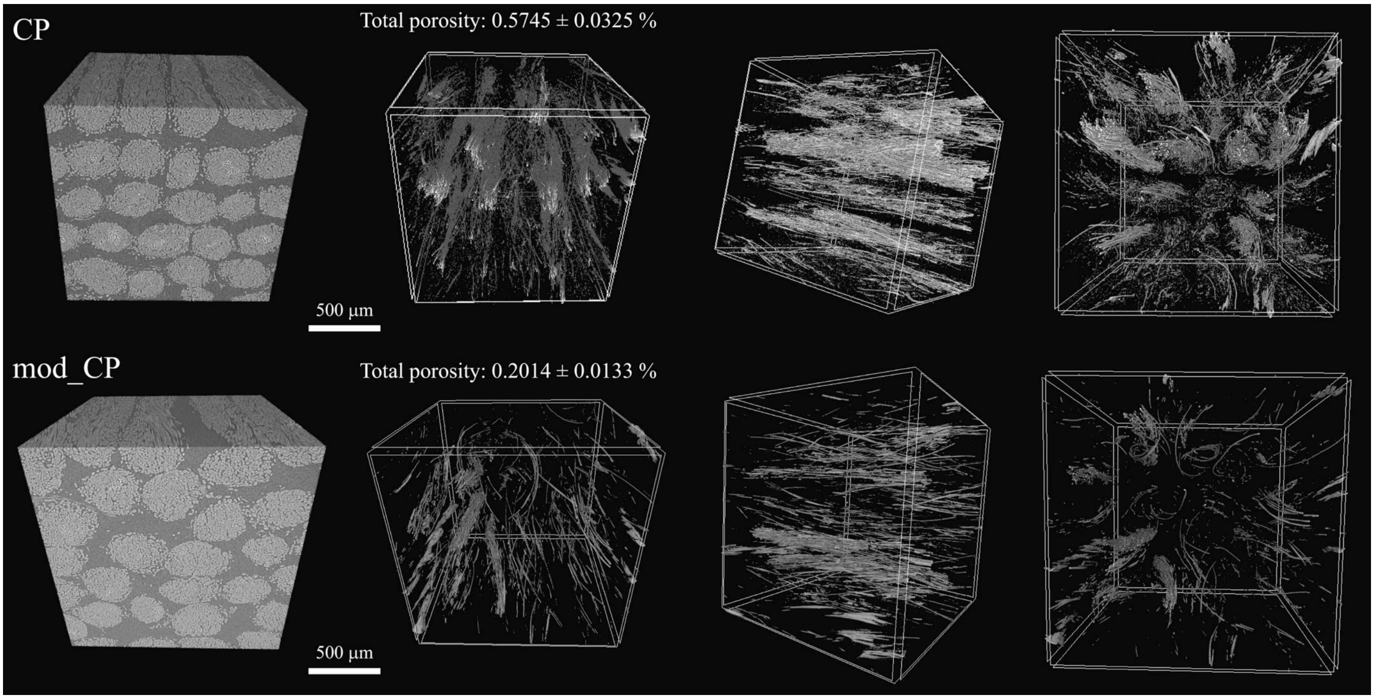

Fig. 6. Three-dimensional reconstructions and visualisation of pores for CP (top) and mod_CP (bottom) matrix FF-composites.

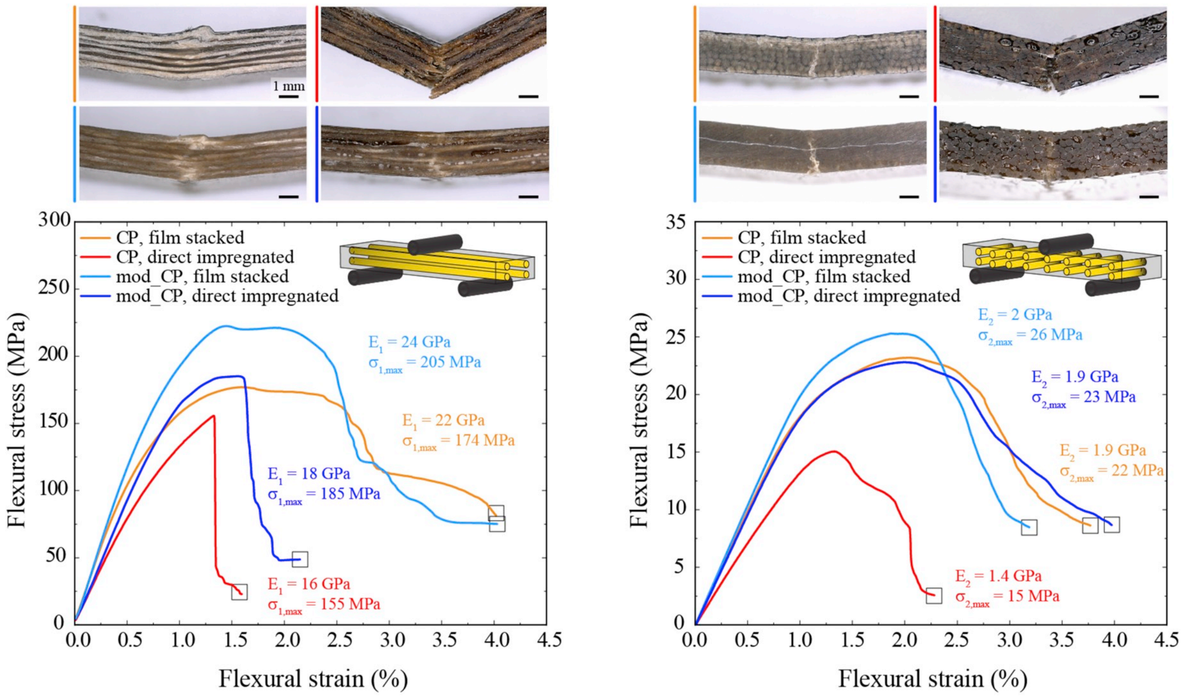

(a) (b)

Fig. 7. Comparison of flexural properties of FF-composites processed via direct impregnation and film stacking. Shows flexural stress-strain curves of composites with CP and mod_CP matrices, tested in (a) longitudinal and (b) transverse direction.

a complete detachment of the two halves of the specimen. In contrast, due to energy absorption via matrix plastic deformation, the thermoplastic composites were still attached after the impact event. The notched properties in the transverse direction show a similar trend to the longitudinal samples. The mod_CP matrix FF-composites exhibited the highest impact strength of 2.8 kJ/m^2, which is ~17% higher compared to composites with CP matrix.

4. Discussion

The blending with Hexamoll and Erucamide enabled disruption of polymer chain entanglements, which affects the polymer's rheological behaviour. For example, the viscosity at low shear rate of mod_CP was reduced to 9% of the initial viscosity of CP (Fig. 2). The viscosity was found to scale linearly with the impregnation time of the fibre preforms. The modelled film stacking impregnation time using mod_CP could be reduced from 6 min to about 0.3 min (Fig. 5). The total surface energy and surface energy components of both CP and mod_CP are very similar (Table 2), suggesting that physical surface interactions were not significantly changed through the polymer modifications. Further, the high work of adhesion estimated for pure CP and flax fibres remained nearly unchanged (Table 2). Due to the lower viscosity, the void content in the composites could be reduced by 65% (Fig. 6), which increases the fibre-matrix contact area and thus allows for a better stress transfer. In addition to lower porosity, shorter processing time prevents degradation of the cellulose in the fibre and the matrix, which also

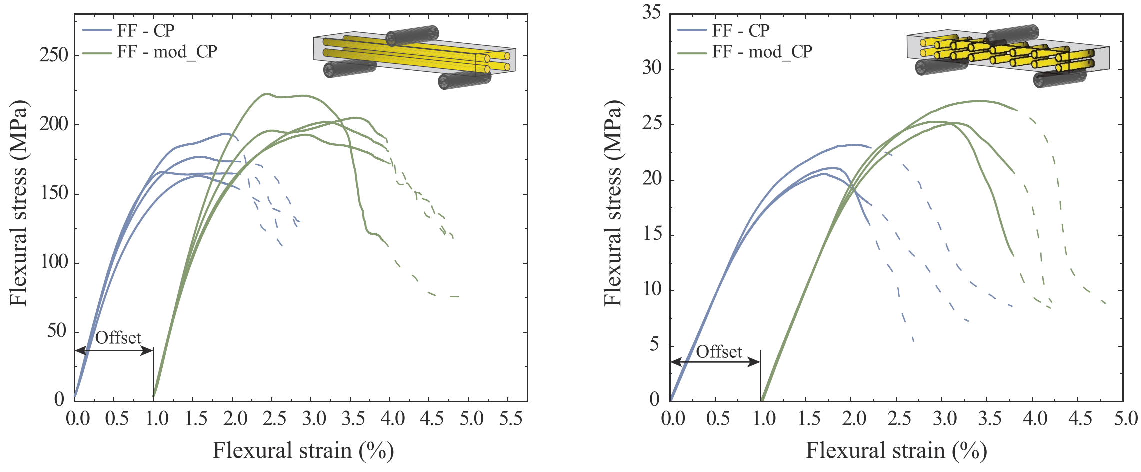

(a) (b)

Fig. 8. Flexural stress-strain curves of film stacked FF-composites with CP (blue) and mod_CP (green) matrices, tested in (a) longitudinal and (b) transverse direction. The strain offset of 1% was integrated to facilitate the comparison of the two sets of curves. (For interpretation of the references to colour in this figure legend, the reader is referred to the Web version of this article.)

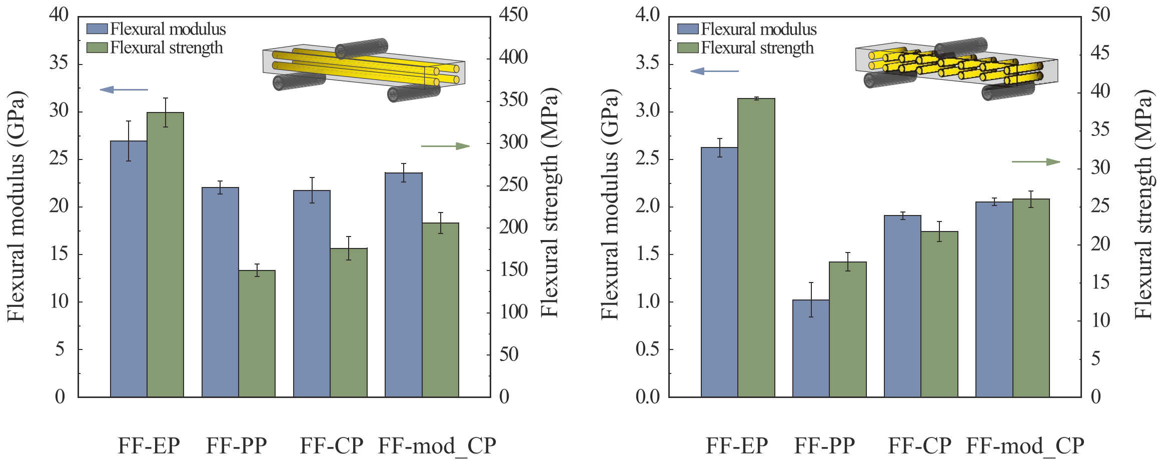

(a) (b)

Fig. 9. Flexural properties of FF-composites. Modulus (blue) and strength (green) in (a) longitudinal and (b) transverse direction. Matrices used are epoxy (EP), polypropylene (PP), cellulose propionate (CP) and modified cellulose propionate (CP_Hex10_Eru02 also referred to as mod_CP). (For interpretation of the references to colour in this figure legend, the reader is referred to the Web version of this article.)

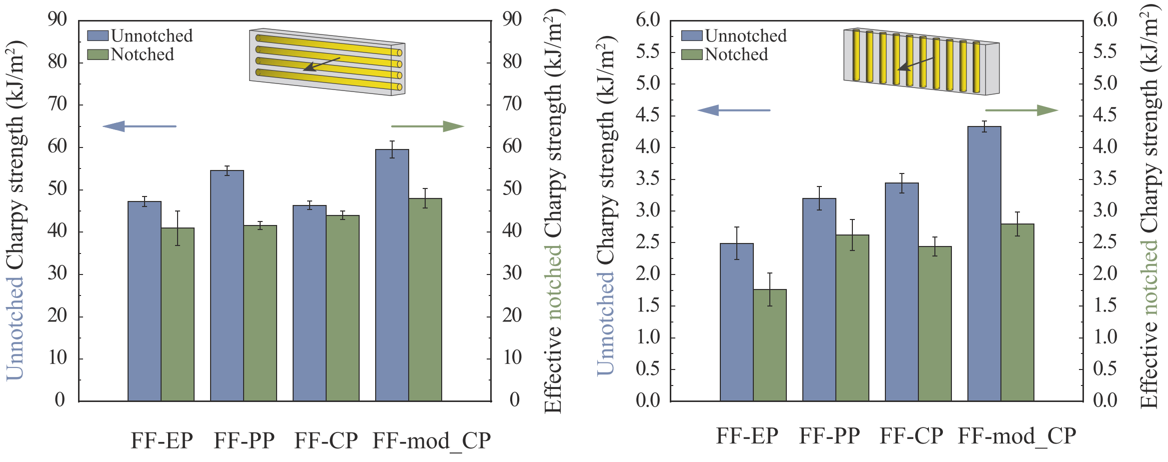

(a) (b)

Fig. 10. Charpy impact strength properties of FF-composites tested in (a) longitudinal (b) transverse fibre direction. The schematics illustrate the testing configuration and the impact direction indicated by the arrow.

increases the mechanical properties of the composite material (Fig. 7). With the utilisation of mod_CP, flexural stiffness and strength could be enhanced in both longitudinal and transverse directions (Figs. 8 and 9). Despite the lower polymer bulk properties of mod_CP, the transverse composite properties were increased. This suggests a better fibre impregnation, which results in a larger contact area, facilitating improved stress transfer compared to the unmodified CP composite. With a longitudinal flexural modulus of 24 GPa the composites developed in this study perform similar compared to Bocell all-cellulose composites reported by Soykeabkaew et al. [7]. When considering the composite flexural properties, CP matrix FF-composites do not yet compete with the EP matrix FF-composites (Fig. 9). Through the combination of low viscosity enabling good impregnation and a strong interface due to the formation of covalent bonds, the EP and flax fibres form composites with high mechanical properties. However, the highly cross-linked molecular structure of EP causes a brittle material behaviour, which does not allow for high energy absorption during impact. Contrarily, the high toughness of the mod_CP was found to translate into a higher toughness of the FF-composite due to the ability of the matrix to deform plastically and the higher resistance against crack propagation. The unnotched composite Charpy strength of 60 kJ/m^2 measured for mod_CP matrix FF-composites is the highest reported for FF-composites with volume fractions above 50 vol%. Overall, the enhancements in composite unnotched and notched toughness were smaller than those that could be achieved for bulk properties due to the poorer impact properties of the fibres.

5. Conclusions

Cellulose propionate (CP) is a naturally derived polymer that can be utilised as matrix materials for all-cellulose composites (ACC) if the CP is modified to reduce its melt viscosity. The reduction was achieved via polymer blending with plasticiser and slip agent additives. The addition of 10 wt% of plasticiser and 2 wt% of slip agent decreased the melt viscosity at low shear rates by 84%. Compromises in tensile stiffness and strength of 22% and 27%, respectively, and a reduction of 10 °C in the glass transition temperature were found to be acceptable for the mod_CP bulk polymer. Therefore, the impact toughness, and in particular the notch sensitivity, was significantly improved. Through the polymer modifications, the unnotched Charpy impact strength could be maintained, whereas the notched strength was increased by 90%. Interestingly, although mod_CP has lower bulk polymer properties compared to the CP base material, the stiffness and strength of flax fibre-reinforced composites could be enhanced by up to 10% and 20%, respectively, through better fibre impregnation and reduced void content. The low melt viscosity not only leads to enhanced mechanical properties but significantly reduces processing times. Without the modifications, the processing of the high viscous CP required higher processing pressures or higher temperatures, to the detriment of degrading the cellulose fibre microstructure and hence the mechanical properties. In addition, the modified composite matrix materials allow for direct impregnation and open the possibility to tailor properties locally by the integration of high modulus and high strength polymer blends for load introduction via additive manufacturing, thermoplastic welding or injection moulding. CP as neat material is composed of up to 45% of cellulose, yet the developed flax fibre-reinforced composites exhibit a combination of high modulus, strength and toughness that are far better than widely used natural fibre-reinforced PP materials and rival state of the art high-performance natural fibre-reinforced composites while remaining bio-based.

Acknowledgements

The authors would like to thank Innosuisse 15091.1 PFIW-IW HIPETCONF and the Swiss Competence Center for Energy Research (Capacity Area A3: Minimization of Vehicular Energy Demand) for funding this study. The contributions of V. Rumpf and A. Bian are gratefully acknowledged and we thank Dr. M. (Grossman) Watson and C. Gosrani for helpful discussions.

References

[1] T. Huber, J. Müssig, O. Curnow, S. Pang, S. Bickerton, M.P. Staiger, A critical review of all-cellulose composites, J. Mater. Sci. 47 (2012) 1171–1186, https://doi.org/10.1007/s10853-011-5774-3.

[2] P. Fratzl, R. Weinkamer, Nature's hierarchical materials, Prog. Mater. Sci. 52 (2007) 1263–1334, https://doi.org/10.1016/j.pmatsci.2007.06.001.

[3] A.K. Mohanty, S. Vivekanandhan, J.M. Pin, M. Misra, Composites from renewable and sustainable resources: challenges and innovations, Science (80-.) 362 (2018) 536–542, https://doi.org/10.1126/science.aat9072.

[4] M. Rueppel, J. Rion, C. Dransfeld, C. Fischer, K. Masania, Damping of carbon fibre and flax fibre angle-ply composite laminates, Compos. Sci. Technol. 146 (2017) 1–9, https://doi.org/10.1016/j.compscitech.2017.04.011.

[5] T. Nishino, K. Takano, K. Nakamae, Elastic modulus of the crystalline regions of cellulose polymorphs, J. Polym. Sci., Part B: Polym. Phys. 33 (1995) 1647–1651, https://doi.org/10.1002/polb.1995.090331110.

[6] M. Frey, G. Biffi, M. Adobes-Vidal, M. Zirkelbach, Y. Wang, K. Tu, A.M. Hirt, K. Masania, I. Burgert, T. Keplinger, Tunable wood by reversible interlocking and bioinspired mechanical gradients, Adv. Sci. 1802190 (2019) 1802190, https://doi.org/10.1002/advs.201802190.

[7] N. Soykeabkaew, T. Nishino, T. Peijs, All-cellulose composites of regenerated cellulose fibres by surface selective dissolution, Compos. Part A Appl. Sci. Manuf. 40 (2009) 321–328, https://doi.org/10.1016/j.compositesa.2008.10.021.

[8] X. Lu, M.Q. Zhang, M.Z. Rong, G. Shi, G.C. Yang, Self-reinforced melt processable composites of sisal, Compos. Sci. Technol. 63 (2003) 177–186, https://doi.org/10.1016/S0266-3538(02)00204-X.

[9] T. Huber, S. Bickerton, J. Müssig, S. Pang, M.P. Staiger, Flexural and impact properties of all-cellulose composite laminates, Compos. Sci. Technol. 88 (2013) 92–98, https://doi.org/10.1016/j.compscitech.2013.08.040.

[10] W. Gindl-Altmutter, J. Keckes, J. Plackner, F. Liebner, K. Englund, M.P. Laborie, All-cellulose composites prepared from flax and lyocell fibres compared to epoxy-matrix composites, Compos. Sci. Technol. 72 (2012) 1304–1309, https://doi.org/10.1016/j.compscitech.2012.05.011.

[11] A.K. Mohanty, A. Wibowo, M. Misra, L.T. Drzal, Effect of process engineering on the performance of natural fiber reinforced cellulose acetate biocomposites, Compos. Part A Appl. Sci. Manuf. 35 (2004) 363–370, https://doi.org/10.1016/j.compositesa.2003.09.015.

[12] B.J.C. Duchemin, A.P. Mathew, K. Oksman, All-cellulose composites by partial dissolution in the ionic liquid 1-butyl-3-methylimidazolium chloride, Compos. Part A Appl. Sci. Manuf. 40 (2009) 2031–2037, https://doi.org/10.1016/j.compositesa.2009.09.013.

[13] T. Nishino, I. Matsuda, K. Hirao, All-cellulose composite, Macromolecules 37 (2004) 7683–7687, https://doi.org/10.1021/ma049300h.

[14] W. Gindl, J. Keckes, All-cellulose nanocomposite, Polymer (Guildf). 46 (2005) 10221–10225, https://doi.org/10.1016/j.polymer.2005.08.040.

[15] C. Gao, L. Yu, H. Liu, L. Chen, Development of self-reinforced polymer composites, Prog. Polym. Sci. 37 (2012) 767–780, https://doi.org/10.1016/j.progpolymsci.2011.09.005.

[16] H. Qi, J. Cai, L. Zhang, S. Kuga, Properties of films composed of cellulose nanowhiskers and a cellulose matrix regenerated from alkali/urea solution, Biomacromolecules 10 (2009) 1597–1602, https://doi.org/10.1021/bm9001975.

[17] W. Woigk, C.A. Fuentes, J. Rion, D. Hegemann, A.W. van Vuure, C. Dransfeld, K. Masania, Interface properties and their effect on the mechanical performance of flax fibre thermoplastic composites, Compos. Part A Appl. Sci. Manuf. 122 (2019) 8–17.

[18] S. Laurenzi, M. Marchetti, Advanced composite materials by resin transfer molding for Aerospace applications, Compos. Their Prop. 2012, pp. 197–226, , https://doi.org/10.5772/2816.

[19] M. Ansell, Natural Fibre Composites and Their Role in Engineering, (2011).

[20] C.A. Fuentes, L.Q.N. Tran, C. Dupont-Gillain, W. Vanderlinden, S. De Feyter, A.W. Van Vuure, I. Verpoest, Wetting behaviour and surface properties of technical bamboo fibres, Colloids Surfaces A Physicochem. Eng. Asp. 380 (2011) 89–99, https://doi.org/10.1016/j.colsurfa.2011.02.032.

[21] C. Della Volpe, M. Brugnara, D. Maniglio, S. Siboni, T. Wangdu, About the possibility of experimentally measuring an equilibrium contact angle and its theoretical and practical consequences, Contact Angle Wettability Adhes 4 (2006) 79–99.

[22] A. Keller, C. Dransfeld, K. Masania, Flow and heat transfer during compression resin transfer moulding of highly reactive epoxies, Compos. B Eng. 153 (2018) 167–175, https://doi.org/10.1016/j.compositesb.2018.07.041.

[23] B. Bachmann, K. Masania, C. Dransfeld, The compression resin transfer moulding process for efficient composite manufacture, Proc. 19th Int. Conf. Compos. Mater. - ICCM19, 2013, pp. 8931–8941.

[24] I. Aranberri-Askargorta, T. Lampke, A. Bismarck, Wetting behavior of flax fibers as reinforcement for polypropylene, J. Colloid Interface Sci. 263 (2003) 580–589, https://doi.org/10.1016/S0021-9797(03)00294-7.

[25] Q. Shen, P. Mikkola, J.B. Rosenholm, Quantitative characterization of the subsurface acid-base properties of wood by XPS and Fowkes theory, Colloids Surfaces A Physicochem. Eng. Asp. 145 (1998) 235–241, https://doi.org/10.1016/S0927-7757(98)00655-4.

[26] C.A. Fuentes, G. Brughmans, L.Q.N. Tran, C. Dupont-Gillain, I. Verpoest, A.W. Van Vuure, Mechanical behaviour and practical adhesion at a bamboo composite interface: physical adhesion and mechanical interlocking, Compos. Sci. Technol. 109 (2015) 40–47, https://doi.org/10.1016/j.compscitech.2015.01.013.

[27] H. Darcy, Les Fontaines Publiques de la Ville de Dijon: Exposition et Application des Principes a Suivre et des Formulesa Employer dans les Questions de Distribution d'Eau, (1856).

[28] J. Studer, C. Dransfeld, J. Jauregui Cano, A. Keller, M. Wink, K. Masania, B. Fiedler, Effect of fabric architecture, compaction and permeability on through thickness thermoplastic melt impregnation, Compos. Part A Appl. Sci. Manuf. 122 (2019) 45–53, https://doi.org/10.1016/j.compositesa.2019.04.008.

[29] R. Umer, S. Bickerton, A. Fernyhough, The effect of yarn length and diameter on permeability and compaction response of flax fibre mats, Compos. Part A Appl. Sci. Manuf. 42 (2011) 723–732, https://doi.org/10.1016/j.compositesa.2011.02.010.